International Journal of Solids and Structures 47 (2010) 2568–2577

Contents lists available at ScienceDirect

International Journal of Solids and Structures

journal homepage: www.elsevier.com/locate/ijsolstr

The G2 constant displacement discontinuity method – Part I: Solution of plane crack problems

G. Exadaktylos *, G. Xiroudakis

Mining Engineering Design Laboratory, Department of Mineral Resources Engineering, Technical University of Crete, GR-73100 Chania, Greece

ARTICLE INFO

Article history:
Available online 24 May 2010

Keywords:
Displacement discontinuity
Strain-gradient elasticity
Crack problems
Stress intensity factors

ABSTRACT

A new constant displacement discontinuity element was presented in a previous paper applied initially for the numerical solution of either isolated straight cracks or for co-linear cracks of the three fundamental deformation modes I, II and III due to the special form of the solution. It was based on the strain-gradient elasticity theory in its simplest possible Grade-2 variant. The assumption of the G2 expression for the stresses has resulted to a better average stress value at the mid-point of the straight displacement discontinuity compared to the classical elasticity solution. This new element gave considerably better predictions of the stress intensity factors compared to the constant displacement discontinuity element and the linear displacement discontinuity element. Moreover, it preserved the simplicity and hence the high speed of computations. In this Part I, the solution for this element is extended for the analysis of cracks of arbitrary shape in an infinite plane isotropic elastic body and it is validated against three known analytical solutions.

1. Introduction

It is common knowledge inside the fracture mechanics community, that even though much achievement has been made in crack modeling techniques, a simple and practical crack modeling technique is still needed, in particular for complex multiple crack growth problems. Crouch (1976a,b) and Crouch and Starfield (1990) by employing the Neuber–Papkovich potential functions corresponding to point dislocations (i.e. displacement discontinuities) has developed such simple and practical technique the so-called displacement discontinuity method (DDM) for solving crack and solid mechanics problems. It is worth mentioning here that DDM may be seen as a special case of the dual Boundary Element Method (BEM) (Chen and Hong, 1999; Hong and Chen, 1988a,b). This method is attractive for researchers and practitioners in the field of Linear Elastic Fracture Mechanics (LEFM) due to its simplicity as compared to cumbersome complex variables theory combined with singular integral equations and numerical integration rules. As was explicitly shown by Crouch (1976a), the assertion that the stress at the centre of a straight constant displacement discontinuity, as is calculated from first principles of the classical linear elasticity theory, represents the average stress over the element, leads to overestimation of displacements at the crack tips and consequently to large errors for the stress intensity factors (SIFs).

Higher order displacement discontinuity elements, as developed by Crawford and Curran (1982), overcome this deficiency and greatly improve the accuracy of the displacement discontinuity method. Crawford and Curran showed that both linear and quadratic displacement discontinuity elements give better results than the constant strength element. In the authors' formulation of the higher order method, however, two (for linear variation of displacement discontinuity) or three (for quadratic variation) collocation points are taken within each element. Thus, the improvement in accuracy comes at the expense of an increase in the number of degrees of freedom in the overall system.

Also, a new formulation of a higher order displacement discontinuity method was subsequently presented by Shou and Crouch (1995) to model two-dimensional elastostatics problems. The new method uses three collocation points for each element, one at the center of the element in question and the others at the centers of the adjacent elements. Each element therefore has a second-order (quadratic) distribution of displacement discontinuity but only two degrees of freedom, which contributes to the efficiency of the approach. By incorporating a special treatment for crack tips, a crack with arbitrary geometry can be modeled. The accuracy of the method was demonstrated by example problems; the results were found to be in good agreement with the analytical solutions and showed that the new method is comparable to the conventional higher order displacement discontinuity method. Also, a special square-root crack tip element developed by Shou and Crouch (1995) that is based on the analytical solutions to crack problems which show that the relative displacement between the crack surfaces is

* Corresponding author. Tel.: +30 28210 37690; fax: +30 28210 37891.
E-mail address: exadakty@mred.tuc.gr (G. Exadaktylos).

0020-7683/$ - see front matter © 2010 Elsevier Ltd. All rights reserved.
doi:10.1016/j.ijsolstr.2010.05.016

proportional to $\sqrt{\xi}$, where ξ is measured from the tip along the crack. In the same paper the analytical formulae for the displacement and stresses of modes I and II crack problems in general plane elasticity were given. Also, the numerical results have shown that the displacement discontinuity modeling technique of a crack with the more elaborate special crack tip elements is very effective.

In a previous work (Exadaktylos and Xiroudakis, 2010a), the above referenced problem was attacked by viewing it from a different perspective. There, the stress at the centre of a straight dislocation was derived from the strain-gradient elasticity theory in its simplest possible Grade-2 (second gradient of strain or G2 theory) variant (Vardoulakis et al., 1996; Exadaktylos et al., 1996; Exadaktylos and Aifantis, 1996; Exadaktylos, 1998, 1999; Exadaktylos and Vardoulakis, 2001). As it was illustrated, the G2 expression for the stresses was derived in a straightforward manner from an averaging procedure that includes the effect of the higher stress gradients along the crack elements especially for those closer to crack tips. This was achieved by recourse to a second-term Taylor's series expansion of the stress around the centre of the DD element. Then, the value of the strain-gradient coefficient or length-scale ℓ that gives the exact agreement of the mid-point displacement of the uniformly pressurized straight displacement discontinuity with the analytical solution for the uniformly pressurized crack, assuming that the latter is discretized with only one element, was easily found. Since the errors of the classical DDM are larger in the regions close to the tips where also the stress distribution along the crack elements display higher gradients, a simple parabolic dependence of the strain-gradient coefficient on the x-coordinate of the centre of the ith element lying along the local Ox-axis along an element was assumed. This G2 formulation applies only on the crack elements and not outside them, where it is assumed that the classical stresses are valid; furthermore, it does not alter the nature of the classical elasticity problem of a cracked body we are aiming to solve. That is to say, no extra boundary conditions along the crack are imposed that are necessary for the solution of a strain-gradient elasticity problem, apart from those prescribed by classical elasticity theory. The efficiency of the new element was demonstrated for the numerical solution of straight or co-linear modes I, II and III crack problems. It was shown that the G2 constant displacement discontinuity (G2CDD) element is stable and gives considerably better predictions of the SIFs compared to the constant displacement discontinuity (CDD) element and better predictions compared to the linear displacement discontinuity (LDD) element presented by Crawford and Curran (1982). Moreover, the new G2 element preserves the simplicity and hence the high speed of computations. However, this first solution presented in Exadaktylos and Xiroudakis (2010a) was not general enough to tackle general plane crack problems due to the special case considered, namely, no variation of crack geometry with respect to the coordinate axis perpendicular to it. In this Part I, the method is extended for the analysis of cracks of arbitrary shape in an infinite plane elastic body as is illustrated in Fig. 1. In Part II (Exadaktylos and Xiroudakis, submitted for publication), the extension of the G2CDD element for the solution of half-plane crack problems, is presented.

2. The general plane G2 solution for arbitrarily inclined straight modes I, II and III dislocations

In this work the following definitions for the normal, in-plane shear and anti-plane strain displacement discontinuity (DD) components for a straight crack lying along Ox-axis are employed

$$\begin{aligned} D_x &\equiv u_x^- - u_x^+, \quad |x| < 1 \\ D_y &\equiv u_y^- - u_y^+, \quad |x| < 1 \\ D_z &\equiv u_z^- - u_z^+, \quad |x| < 1 \end{aligned} \tag{1}$$

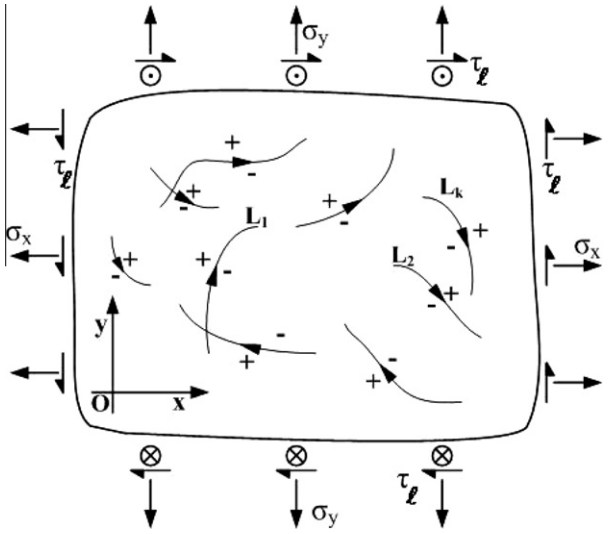

Fig. 1. A plane isotropic elastic body containing isolated or mutually intersecting cracks $L_1, L_2, \ldots, L_k$ and subjected to normal stresses σ_x, σ_y and shear stress τ_ℓ at infinity.

where u_x, u_y, u_z denote the displacements along Ox-, Oy- and Oz-axes, respectively, of an $Oxyz$ Cartesian coordinate system, and $y = 0^-$, $y = 0^+$ denote the negative and positive sides of the line segment in question. Also, hereafter tensile stresses are considered as positive quantities and the unit length is chosen to be the half-width of the DD element since the sizes of the elements are taken to be equal.

The approach in Exadaktylos and Xiroudakis (2010a) was to change the boundary value problem of a mode I, II or III straight crack with prescribed shape in an infinite strain-gradient or G2 solid into one of a semi-infinite G2 solid by exploiting the symmetry of the stress fields, produced by the three fundamental displacement modes, about the line $y = 0$ (Sneddon and Lowengrub, 1969). The upper half-plane $y \geqslant 0$ solution for the stresses in plane-strain produced by a mode I dislocation occupying the line segment $-1 < x < 1$, $y = 0^{\pm}$ with no loading at infinity and displaying a constant DD of magnitude D_y may be found by recourse to the Fourier transform technique as follows (Exadaktylos and Xiroudakis, 2010a)

$$\begin{aligned} \sigma_{xx}^{\mathrm{I}}(x,y) = &-\frac{GD_y}{2(1-\nu)}\sqrt{\frac{2}{\pi}}\int_0^\infty \xi^{1/2}(1-\ell^2\xi^2) \\ &\times (1-y\xi)J_{1/2}(\xi)e^{-y\xi}\cos x\xi\, d\xi \end{aligned} \tag{2a}$$

$$\sigma_{xy}^{\mathrm{I}}(x,y) = -\frac{GD_y}{2(1-\nu)}y\sqrt{\frac{2}{\pi}}\int_0^\infty \xi^{3/2}(1-\ell^2\xi^2)J_{1/2}(\xi)e^{-y\xi}\sin x\xi\, d\xi \tag{2b}$$

$$\begin{aligned} \sigma_{yy}^{\mathrm{I}}(x,y) = &-\frac{GD_y}{2(1-\nu)}\sqrt{\frac{2}{\pi}}\int_0^\infty \xi^{1/2}(1-\ell^2\xi^2) \\ &\times (1+y\xi)J_{1/2}(\xi)e^{-y\xi}\cos x\xi\, d\xi \end{aligned} \tag{2c}$$

where the Latin superscript "I" designates a mode I dislocation, G, ν denote the shear modulus and Poisson's ratio, respectively, of the material, ℓ is the strain-gradient coefficient that has dimensions of length, and $J_n(\cdot)$ is the usual Bessel function of the first kind and of order n. By recourse to analytical expressions of the above semi-infinite integrals (Gradshteyn and Ryzhik, 1980), the following analytical expressions for the stresses may be subsequently derived

$$\sigma^{\mathrm{I}}_{xx}(x,y)=\frac{G}{2\pi(1-\nu)}\left[\frac{x-1}{y^2+(x-1)^2}-\frac{x+1}{y^2+(x+1)^2}-2y^2\left(\frac{x-1}{\left(y^2+(x-1)^2\right)^2}-\frac{x+1}{(y^2+(x+1)^2)^2}\right)+2\ell^2\left\{\frac{x-1}{(y^2+(x-1)^2)^2}-\frac{x+1}{(y^2+(x+1)^2)^2}-16y^2\left(\frac{x-1}{(y^2+(x-1)^2)^3}-\frac{x+1}{(y^2+(x+1)^2)^3}\right)+24y^4\left(\frac{x-1}{(y^2+(x-1)^2)^4}-\frac{x+1}{(y^2+(x+1)^2)^4}\right)\right\}\right]D_y \tag{3a}$$

$$\sigma^{\mathrm{I}}_{xy}(x,y)=\frac{G}{2\pi(1-\nu)}y\left[\frac{1}{y^2+(x-1)^2}-\frac{1}{y^2+(x+1)^2}-2y^2\left(\frac{1}{(y^2+(x-1)^2)^2}-\frac{1}{(y^2+(x+1)^2)^2}\right)+6\ell^2\left\{\frac{1}{(y^2+(x-1)^2)^2}-\frac{1}{(y^2+(x+1)^2)^2}-8y^2\left(\frac{1}{(y^2+(x-1)^2)^3}-\frac{1}{(y^2+(x+1)^2)^3}\right)+8y^4\left(\frac{1}{(y^2+(x-1)^2)^4}-\frac{1}{(y^2+(x+1)^2)^4}\right)\right\}\right]D_y \tag{3b}$$

$$\sigma^{\mathrm{I}}_{yy}(x,y)=\frac{G}{2\pi(1-\nu)}\left[\frac{x-1}{y^2+(x-1)^2}-\frac{x+1}{y^2+(x+1)^2}+2y^2\left(\frac{x-1}{(y^2+(x-1)^2)^2}-\frac{x+1}{(y^2+(x+1)^2)^2}\right)+2\ell^2\left\{\frac{x-1}{(y^2+(x-1)^2)^2}-\frac{x+1}{(y^2+(x+1)^2)^2}+8y^2\left(\frac{x-1}{(y^2+(x-1)^2)^3}-\frac{x+1}{(y^2+(x+1)^2)^3}\right)-24y^4\left(\frac{x-1}{(y^2+(x-1)^2)^4}-\frac{x+1}{(y^2+(x+1)^2)^4}\right)\right\}\right]D_y \tag{3c}$$

In a similar fashion, the upper half-plane $y\geqslant 0$ plane-strain boundary value problem of a mode II dislocation occupying the line segment $-\alpha<x<\alpha$, $y=0$ with no loading at infinity and with a prescribed shape of a constant DD of magnitude D_x has the following solution (Exadaktylos and Xiroudakis, 2010a)

$$\sigma^{\mathrm{II}}_{xx}(x,y)=-\frac{GD_x}{2(1-\nu)}\sqrt{\frac{2}{\pi}}\int_0^\infty \xi^{1/2}(1-\ell^2\xi^2)\times(2-y\xi)J_{1/2}(\xi)e^{-y\xi}\sin x\xi\,d\xi \tag{4a}$$

$$\sigma^{\mathrm{II}}_{xy}(x,y)=-\frac{GD_x}{2(1-\nu)}\sqrt{\frac{2}{\pi}}\int_0^\infty \xi^{1/2}(1-\ell^2\xi^2)\times(1-y\xi)J_{1/2}(\xi)e^{-y\xi}\cos x\xi\,d\xi \tag{4b}$$

$$\sigma^{\mathrm{II}}_{yy}(x,y)=-\frac{GD_x}{2(1-\nu)}\sqrt{\frac{2}{\pi}}y\int_0^\infty \xi^{3/2}(1-\ell^2\xi^2)J_{1/2}(\xi)e^{-y\xi}\sin x\xi\,d\xi \tag{4c}$$

where the superscript "II" designates the mode II or in-plane shear dislocation. Again, the analytical evaluation of the above integral expressions for the stresses has as follows

$$\sigma^{\mathrm{II}}_{xx}(x,y)=\frac{Gy}{2\pi(1-\nu)}\left[\frac{-3}{y^2+(x-1)^2}-\frac{-3}{y^2+(x+1)^2}+2y^2\left(\frac{1}{(y^2+(x-1)^2)^2}-\frac{1}{(y^2+(x+1)^2)^2}\right)+2\ell^2\left\{\frac{-9}{(y^2+(x-1)^2)^2}-\frac{-9}{(y^2+(x+1)^2)^2}+32y^2\left(\frac{1}{(y^2+(x-1)^2)^3}-\frac{1}{(y^2+(x+1)^2)^3}\right)-24y^4\left(\frac{1}{(y^2+(x-1)^2)^4}-\frac{1}{(y^2+(x+1)^2)^4}\right)\right\}\right]D_x \tag{5a}$$

$$\sigma^{\mathrm{II}}_{xy}(x,y)=\frac{G}{2\pi(1-\nu)}\left[\frac{x-1}{y^2+(x-1)^2}-\frac{x+1}{y^2+(x+1)^2}-2y^2\left(\frac{x-1}{(y^2+(x-1)^2)^2}-\frac{x+1}{(y^2+(x+1)^2)^2}\right)+2\ell^2\left\{\frac{x-1}{(y^2+(x-1)^2)^2}-\frac{x+1}{(y^2+(x+1)^2)^2}-16y^2\left(\frac{x-1}{(y^2+(x-1)^2)^3}-\frac{x+1}{(y^2+(x+1)^2)^3}\right)+24y^4\left(\frac{x-1}{(y^2+(x-1)^2)^4}-\frac{x+1}{(y^2+(x+1)^2)^4}\right)\right\}\right]D_x \tag{5b}$$

$$\sigma^{\mathrm{II}}_{yy}(x,y)=\frac{G}{2\pi(1-\nu)}\frac{y}{a}\left[\frac{1}{y^2+(x-1)^2}-\frac{1}{y^2+(x+1)^2}-2y^2\left(\frac{1}{(y^2+(x-1)^2)^2}-\frac{1}{(y^2+(x+1)^2)^2}\right)+6\ell^2\left\{\frac{1}{(y^2+(x-1)^2)^2}-\frac{1}{(y^2+(x+1)^2)^2}-8y^2\left(\frac{1}{(y^2+(x-1)^2)^3}-\frac{1}{(y^2+(x+1)^2)^3}\right)+8y^4\left(\frac{1}{(y^2+(x-1)^2)^4}-\frac{1}{(y^2+(x+1)^2)^4}\right)\right\}\right]D_x \tag{5c}$$

Finally, the upper half-plane $y\geqslant 0$ problem of mode III (anti-plane strain) dislocation occupying the line segment $|x|\leqslant 1$, $y=0$ with a prescribed constant DD equal to D_z has the following solution (Exadaktylos and Xiroudakis, 2010a)

$$\begin{aligned}\sigma^{\mathrm{III}}_{xz}(x,y)&=-\frac{GD_z}{2}\sqrt{\frac{2}{\pi}}\int_0^\infty \xi^{1/2}(1-\ell^2\xi^2)J_{1/2}(\xi)e^{-y\xi}\sin x\xi\,d\xi,\\ \sigma^{\mathrm{III}}_{yz}(x,y)&=-\frac{GD_z}{2}\sqrt{\frac{2}{\pi}}\int_0^\infty \xi^{1/2}(1-\ell^2\xi^2)J_{1/2}(\xi)e^{-y\xi}\cos x\xi\,d\xi.\end{aligned} \tag{6}$$

where the superscript "III" designates the mode III dislocation. Finally, the evaluations of the above semi-infinite integrals for this case explicitly give

$$\sigma^{\mathrm{III}}_{xz}(x,y)=-\frac{G}{\pi}y\left[\frac{1}{y^2+(x-1)^2}-\frac{1}{y^2+(x+1)^2}+2\ell^2\left\{\frac{3}{(y^2+(x-1)^2)^2}-\frac{3}{(y^2+(x+1)^2)^2}-4y^2\left(\frac{1}{(y^2+(x-1)^2)^3}-\frac{1}{(y^2+(x+1)^2)^3}\right)\right\}\right]D_z \tag{7a}$$

$$\sigma_{yz}^{III}(x,y) = -\frac{G}{\pi}\left[\frac{x-1}{y^2+(x-1)^2} - \frac{x+1}{y^2+(x+1)^2} + 2\ell^2\left\{-\left(\frac{x-1}{(y^2+(x-1)^2)^2} - \frac{x+1}{(y^2+(x+1)^2)^2}\right) - 4y^2\left(\frac{x-1}{(y^2+(x-1)^2)^3} - \frac{x+1}{(y^2+(x+1)^2)^3}\right)\right\}\right] D_z \quad (7b)$$

Next, by virtue of the principle of superposition, the general mixed modes I and II plane-strain linear elastic solutions, as well as the mode III solution may be found as follows,

$$\sigma_{xx}(x,y) = \sigma_{xx}^{II}(x,y) + \sigma_{xx}^{I}(x,y) = A_{xx}^{II}(x,y)D_x + A_{xx}^{I}(x,y)D_y \quad (8a)$$

$$\sigma_{xy}(x,y) = \sigma_{xy}^{II}(x,y) + \sigma_{xy}^{I}(x,y) = A_{xy}^{II}(x,y)D_x + A_{xy}^{I}(x,y)D_y \quad (8b)$$

$$\sigma_{yy}(x,y) = \sigma_{yy}^{II}(x,y) + \sigma_{yy}^{I}(x,y) = A_{yy}^{II}(x,y)D_x + A_{yy}^{I}(x,y)D_y \quad (8c)$$

$$\sigma_{xz}(x,y) = \sigma_{xz}^{III}(x,y) = A_{xz}^{III}(x,y)D_z \quad (8d)$$

$$\sigma_{yz}(x,y) = \sigma_{yz}^{III}(x,y) = A_{yz}^{III}(x,y)D_z \quad (8e)$$

where the influence coefficients A_{xx}^{I}, A_{xy}^{I}, A_{yy}^{I}, A_{xx}^{II}, A_{xy}^{II}, A_{yy}^{II}, A_{xz}^{III}, A_{yz}^{III} may be easily derived from Eqs. (2)–(8) by dividing the expressions for the stresses with the appropriate DD's. As was originally illustrated by Crouch (1976a,b) and Crouch and Starfield (1990), the above stress solution for constant normal, transverse or screw displacement discontinuities over a finite line segment, can be used to develop a numerical procedure for solving complex boundary value problems in elasticity. This special boundary element procedure, the so-called CDD method, consists simply of placing N displacement discontinuities of unknown magnitude and of equal length along the boundaries of the region to be analyzed, then setting up and solving a system of algebraic equations to find the discontinuity values that produce prescribed boundary tractions or displacements. For easy reference, this procedure is outlined in the next section.

3. Numerical procedure for a system of curvilinear cracks

The purpose here is to find the new influence coefficients for the case that the elementary line discontinuities have arbitrary orientation, and finally to set up the equations of the stress boundary value problem. It is convenient for this purpose to describe each displacement discontinuity with reference to a local transformed coordinate system $O\bar{x}\bar{y}$ attached to it, as is illustrated in Fig. 2. This local system results from the global coordinate system Oxy after applying a translation and then a rotation. The components of the translation are x_0, y_0, whereas the rotation is defined by the angle β positive in the counterclockwise sense as is shown in Fig. 2. Hence, this coordinate transformation may be specified as follows

$$\bar{x} = (x-x_0)\cos\beta + (y-y_0)\sin\beta$$
$$\bar{y} = -(x-x_0)\sin\beta + (y-y_0)\cos\beta \quad (9)$$

As is illustrated in Fig. 3a the local coordinates of point (i), located at the centre of the ith linear segment, relative to the jth element are given by the formulae

$$\bar{x}_j = (x_i-x_j)\cos\beta_j + (y_i-y_j)\sin\beta_j$$
$$\bar{y}_j = -(x_i-x_j)\sin\beta_j + (y_i-y_j)\cos\beta_j \quad (10)$$

Subsequently, the stresses at the mid-point of the ith element due to shear and normal displacement discontinuities of the jth element (e.g. Fig. 3b) referred to the jth local coordinate system, could be easily found from relationships (8) and (10) as follows

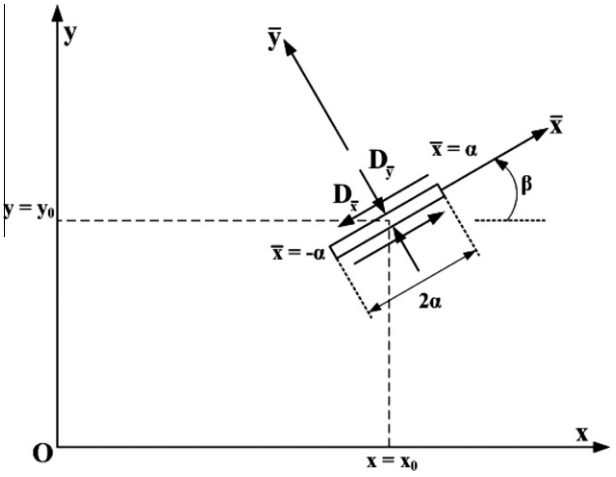

Fig. 2. Global and local coordinate systems for the problem of normal and shear constant displacement discontinuities over an arbitrarily oriented, finite line segment in an infinite body and notations.

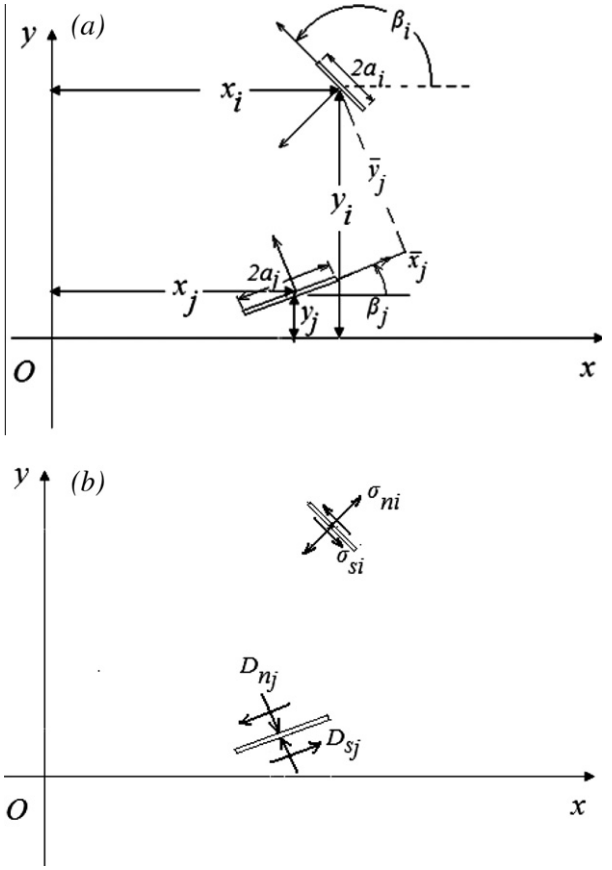

Fig. 3. (a) Local coordinates of ith DD element with respect to the jth element, and (b) influence of DD's of the jth element on the stresses of the ith element.

$$\sigma_{nij} = A_{yy}^{II}(\bar{x}_j,\bar{y}_j)D_{sj} + A_{yy}^{I}(\bar{x}_j,\bar{y}_j)D_{nj}$$
$$\sigma_{sij} = A_{xy}^{II}(\bar{x}_j,\bar{y}_j)D_{sj} + A_{xy}^{I}(\bar{x}_j,\bar{y}_j)D_{nj}$$
$$\sigma_{tij} = A_{xx}^{II}(\bar{x}_j,\bar{y}_j)D_{sj} + A_{xx}^{I}(\bar{x}_j,\bar{y}_j)D_{nj}$$
$$\sigma_{tzij} = A_{xz}(\bar{x}_j,\bar{y}_j)D_{zj}$$
$$\sigma_{szij} = A_{yz}(\bar{x}_j,\bar{y}_j)D_{zj} \quad (11)$$

where we have changed the notation for the local coordinates of a given DD segment in such a manner that hereafter *Os*-axis corresponds to $O\bar{x}$-axis and *On*-axis to $O\bar{y}$-axis, and the subscript "*t*" denotes the tangential stress component directed along the line segment for modes I and II dislocations and along *Oz*-axis for mode III dislocations.

The general stress equations for the DD method are obtained from the foregoing results by considering an infinite body containing *N* line segments, arbitrarily oriented with respect to the global *Oxy* coordinate system. Then, the total stresses imparted to the *i*th element referred to its local coordinate system due to the DD's of all the *N* linear segments, may be found by the superposition of the stresses caused individually from each segment by recourse to Eq. (11) and then by the application of two consecutive rotations of coordinates one clockwise with an angle β_j and another counterclockwise at an angle β_i as follows

$$\begin{aligned}
\sigma_{ti} &= \sum_{j=1}^{N}\Big\{\sigma_{tij}\cos(\beta_j-\beta_i)^2-\sigma_{sij}\sin(2(\beta_j-\beta_i)) \\
&\qquad +\sigma_{nij}\sin(\beta_j-\beta_i)^2\Big\} \\
\sigma_{si} &= \sum_{j=1}^{N}\{0.5(\sigma_{tij}-\sigma_{nij})\sin(2(\beta_j-\beta_i)) \\
&\qquad +\sigma_{sij}\cos(2(\beta_j-\beta_i))\} \\
\sigma_{ni} &= \sum_{j=1}^{N}\Big\{\sigma_{tij}\sin(\beta_j-\beta_i)^2+\sigma_{sij}\sin(2(\beta_j-\beta_i)) \\
&\qquad +\sigma_{nij}\cos(\beta_j-\beta_i)^2\Big\} \\
\sigma_{tzi} &= \sum_{j=1}^{N}\{-\sigma_{szij}\sin(\beta_j-\beta_i)+\sigma_{tzij}\cos(\beta_j-\beta_i)\} \\
\sigma_{szi} &= \sum_{j=1}^{N}\{\sigma_{tzij}\sin(\beta_j-\beta_i)+\sigma_{szij}\cos(\beta_j-\beta_i)\}
\end{aligned} \tag{12}$$

Finally, from the above relations a $3N\times 3N$ algebraic system of linear equations with unknowns the DD components, namely D_{si}, D_{ni}, D_{zi} ($i=1,\ldots,N$), could be formed for the solution of Newmann or the so-called "first fundamental" boundary value problem by substituting the stress boundary conditions $\sigma_{si}=(\sigma_{si})_0$, $\sigma_{ni}=(\sigma_{ni})_0$ regarding plane mixed modes I, II problems and $\sigma_{szi}=(\sigma_{szi})_0$ regarding anti-plane mode III crack problems ($i=1,\ldots,N$), where subscript "0" denotes a known stress value along the *i*th line segment, i.e.

$$\begin{aligned}
(\sigma_{ni})_0 &= \sum_{j=1}^{N}\{A_{nsij}D_{sj}+A_{nnij}(x,y)D_{nj}\} \\
(\sigma_{si})_0 &= \sum_{j=1}^{N}\{A_{ssij}D_{sj}+A_{snij}(x,y)D_{nj}\} \\
(\sigma_{szi})_0 &= \sum_{j=1}^{N}A_{szij}D_{zj}
\end{aligned} \tag{13}$$

where A_{nsij}, A_{nnij}, A_{ssij}, A_{snij}, A_{szij} ($i,j=1,\ldots,N$) denote influence coefficients for the stresses. Explicit expressions for these influence coefficients could be written, but they clearly would be lengthy. It is preferable simply to evaluate the coefficients within a computer program according to the process defined above.

4. Validation of the theory with closed-form solutions for plane crack problems

Problems involving an infinite body with cracks – even intersecting cracks – subjected to complex loading conditions, are solved almost trivially by the DD method. Each crack is divided into a series of segments over which stress boundary conditions are known, and Eqs. (13) are solved for the discontinuity components at each segment. Stresses elsewhere in the body then can be computed by Eqs. (12) by summing the contributions of all the individual discontinuities.

One of the main objectives of many analyses of crack problems in the context of LEFM is to obtain values of the SIFs K_{I}, K_{II}, K_{III} at the crack tips. A simple way of accomplishing this is to use the known LEFM relationships

$$\begin{aligned}
K_{\mathrm{I}} &= -\frac{G}{4(1-\nu)}\lim_{r\to 0}\left\{\sqrt{\frac{2\pi}{r}}D_y(r)\right\} \\
K_{\mathrm{II}} &= -\frac{G}{4(1-\nu)}\lim_{r\to 0}\left\{\sqrt{\frac{2\pi}{r}}D_x(r)\right\} \\
K_{\mathrm{III}} &= -\frac{G}{4}\lim_{r\to 0}\left\{\sqrt{\frac{2\pi}{r}}D_z(r)\right\}
\end{aligned} \tag{14}$$

where the negative sign is due to the adopted sign convention for the DD's and stresses, $D_y(r)$, $D_x(r)$, $D_z(r)$ are the normal, shear and anti-plane shear components of displacement discontinuity a distance *r* from the crack tip(s). For practical purposes, the limits in Eqs. (14) can be approximated by evaluating the expressions for a fixed value of *r*, small in relation to the size of the crack. The SIFs are simply calculated numerically by using the displacement discontinuity at the mid-points of the crack-tip cracks. Thus, accurate values of SIFs may be obtained if the DD distributions in the vicinity of the crack tip(s) are known accurately.

Eqs. (3), (5) and (7)–(13) were implemented into a computer code called G2TWODD (i.e. acronym for G2 two-dimensional displacement discontinuity code) that is dedicated for fast calculations of SIFs and stresses of cracked elastic bodies. In this section, three indicative numerical examples are presented to illustrate the improved accuracy referring to the determination of SIFs with the special G2CDD element when compared with the CDD element, with the higher-order linear displacement discontinuity (LDD) element presented by Crawford and Curran (1982), and with the special crack-tip displacement discontinuity (SCDD) element (i.e. Shou and Crouch, 1995).

4.1. Case 1: Periodic array of parallel straight cracks

The first case pertains to the infinite row of periodic parallel straight cracks subjected to far-field tension and anti-plane shear tractions, as it is illustrated in Fig. 4. The relative distance of cracks may be defined as follows

$$s=\frac{a}{a+h}=\frac{1}{1+\frac{h}{a}} \tag{15}$$

It may be seen from the above definition (15) that as $h\to\infty$ then $s\to 0$, whereas as $h\to 0$ then $s\to 1$. Also, the SIFs for the problem at hand may be expressed in the following manner

$$\begin{Bmatrix} K_{\mathrm{I}} \\ K_{\mathrm{III}} \end{Bmatrix} = \begin{Bmatrix} \sigma \\ \tau_\ell \end{Bmatrix}\sqrt{\pi a}\begin{Bmatrix} F_{\mathrm{Is}} \\ F_{\mathrm{IIIs}} \end{Bmatrix} \tag{16}$$

where F_{Is}, F_{IIIs} are configuration correction factors for the two cases of modes I and III, respectively, with known dependencies w.r.t. the relative distance *s* (Tada et al., 1973).

From Fig. 5a it may be seen that as the number of discretization elements per crack increases, the dimensionless mode I SIF ($K_{\mathrm{I}}/(\sigma\sqrt{a})$) predicted by the G2CDD method converges to the analytical solution. It is noted that SIF of a crack is calculated from the two crack tip elements by recourse to the first of Eq. (14) with *r* equal to the half element length. Moreover, the G2CDD gives always a better prediction compared to the other two methods, namely CDD and LDD, whereas LDD predictions are much better than CDD. Fig. 5b shows the variation of the dimensionless mode I SIF predicted by

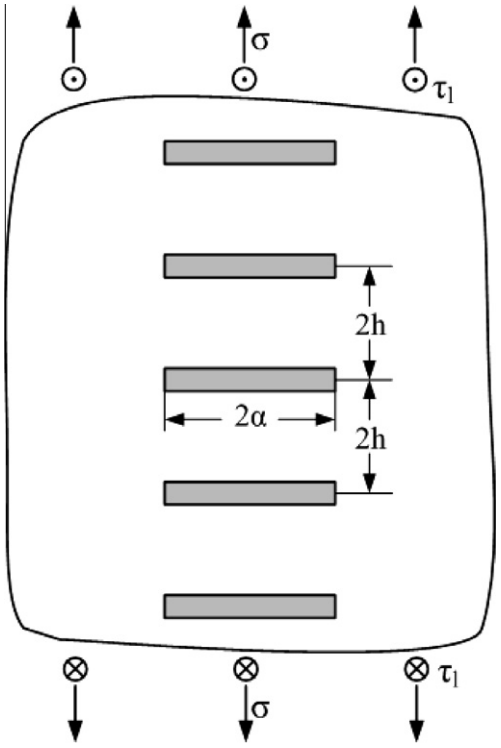

Fig. 4. Periodic array of parallel straight cracks in an infinite solid subjected to far-field uniaxial tensile stress and anti-plane shear stress.

the three numerical methods and by the analytical solution, as the relative crack distance increases. Also, LDD and CDD do not converge to the true solution with increasing number of elements since as the element size reduces the mid-point of crack tip elements approach the actual crack tips. Finally, the relative errors (relative error = (computed value − analytical value)/analytical value × 100) of the three distinct numerical methods with increasing number of elements for fixed relative crack distance $s = 0.5$, and with increasing relative crack distance for a fixed number of discretization elements per crack ($N = 50$) are graphically presented in Fig. 5c and d, respectively. From these figures the much better accuracy and convergence of the G2CDD compared to the CDD and LDD methods may be observed. It is further noticed here that similar conclusions have been drawn for the behavior of mode III SIF for the case of far-field anti-plane shear traction.

4.2. Case 2: The symmetrical star crack

Next, we consider the symmetrical star crack configuration subjected to a far-field all-around uniform tension, as it is shown in Fig. 6. Due to symmetry, the only surviving SIF is the mode I that is acting on the non-common tips of the cracks since there is no stress concentration at the common crack tips. The SIF is given by the following abridged form

$$K_I = \sigma\sqrt{\pi a}F(n), \quad n \geqslant 2 \tag{17}$$

wherein $F(n)$ is the corresponding configuration correction factor given w.r.t. the number of radial cracks n (Tada et al., 1973). The following approximate formula holds true in this case

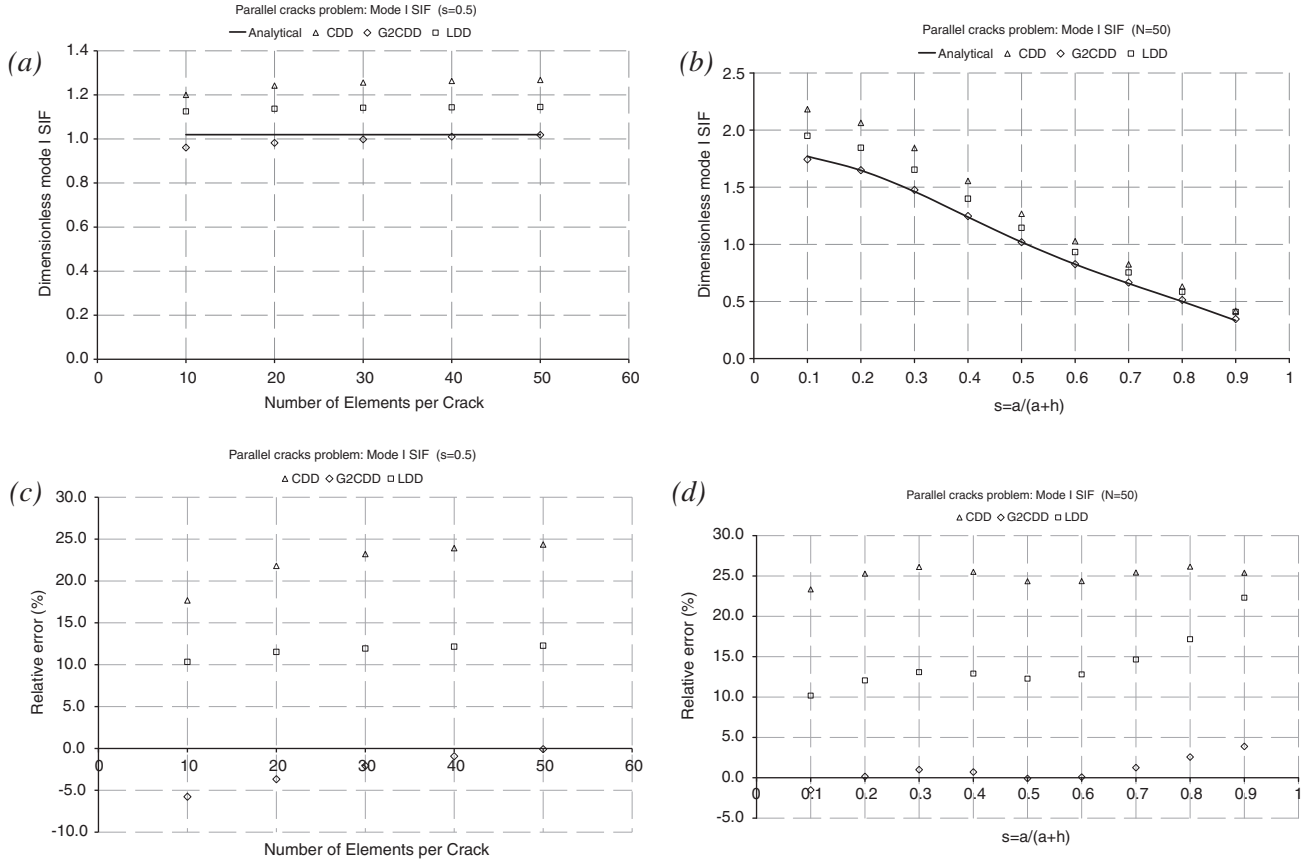

Fig. 5. Variation of the dimensionless SIF (i.e. $K_I/(\sigma\sqrt{a})$) predicted by the analytical solution and the three distinct displacement discontinuity techniques with (a) the number of elements per crack for a fixed relative distance between the cracks and (b) with the relative distance s of cracks for fixed number of elements per crack ($N = 50$), and variation of relative error of SIF with respect to (c) number of elements per crack and fixed relative distance, and (d) the relative distance of cracks for fixed number of elements per crack.

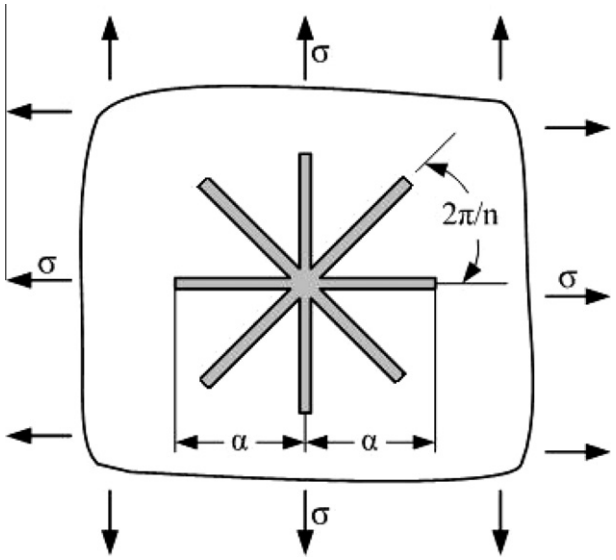

Fig. 6. Radial straight cracks of equal length emanating from a common point in an infinite solid subjected to far-field biaxial tension.

$$F(n) \approx \frac{2}{\sqrt{n}}, \quad n \geqslant 10 \tag{18}$$

First it should be noted here that the existence of a node common to all the elements at the central intersection point of the star crack system, is possible only for an even number of cracks due to symmetry arguments. For this particular case a common node at the centre was not applied, since cases of odd number of cracks

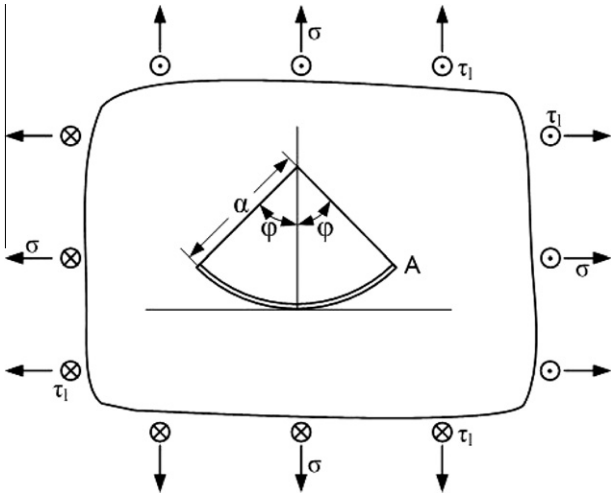

Fig. 8. The curved crack which is a part of a circle in an infinite isotropic plane subjected to biaxial tensile and anti-plane shear stresses.

have been also examined. The comparison of the effectiveness of the three numerical methods, namely the CDD, G2CDD and LDD, in computing the mode I SIF at the crack tips for various values of discretization elements and radial cracks, may be seen in Fig. 7a–d. This example also illustrates the effectiveness of the G2CDD method compared to the other two methods for the calculation of the SIF. Fig. 7a displays the convergence of the three techniques with increasing number of elements for the case of $n = 6$, whereas Fig. 7b presents the comparison of the numerical predictions of the three methods with the respective analytical solution

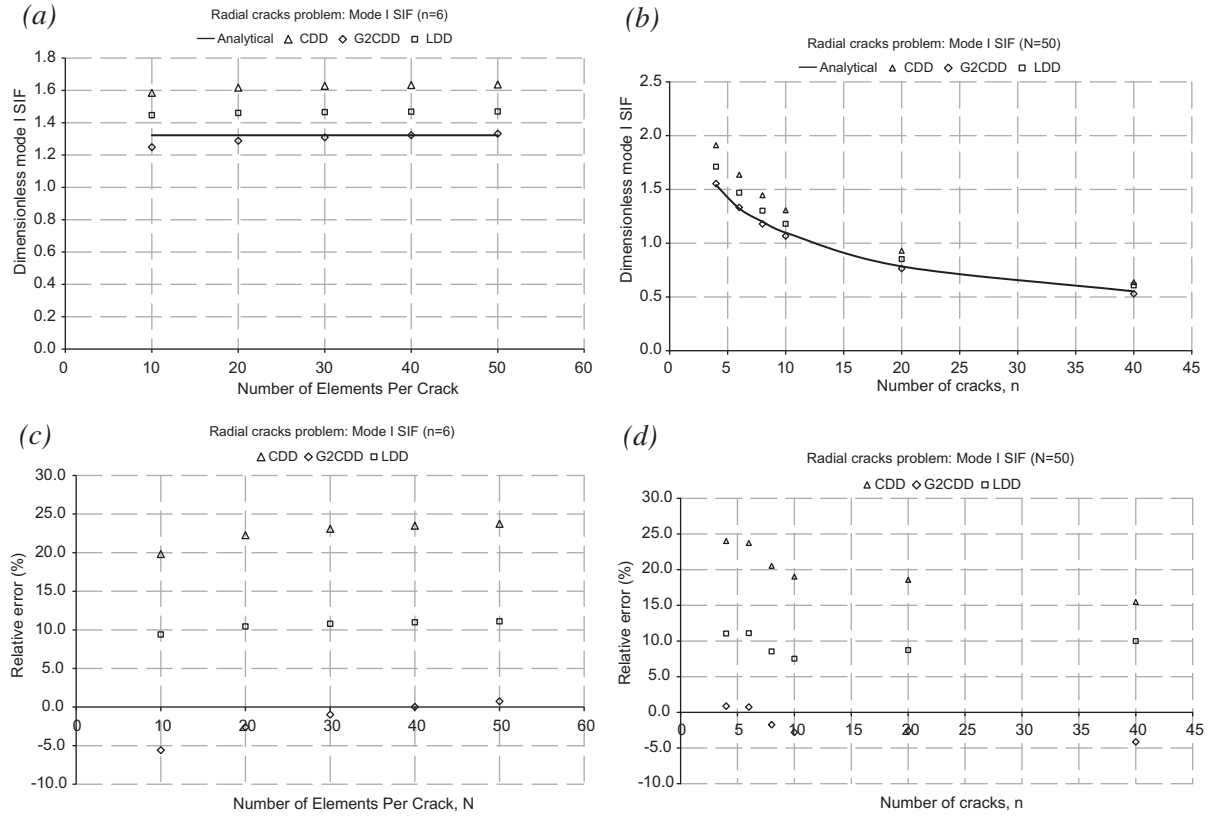

Fig. 7. Variation of the dimensionless SIF (i.e. $K_I/(\sigma\sqrt{a})$) predicted by the analytical solution and the three distinct displacement discontinuity techniques with (a) the number of elements per crack for six radial cracks, and (b) with the number of cracks for fixed number of elements per crack (number of elements per crack $N = 50$) and; variation of relative error of SIF with respect to (c) number of elements per crack for a fixed number of radial cracks, and (d) the number of radial cracks for fixed number of elements per crack.

for $N = 50$ elements per crack and for various number of radial cracks, n. The relative errors of the three methods are also graphically presented in Fig. 7c and d as the discretization density and number of cracks increases, respectively. From Fig. 7c it may be observed that G2CDD method gives the smaller relative error, while convergence to the analytical solution is not possible since for larger number of elements the closer at the tip is the node of the crack tip element. It is worth noticing from Fig. 7d that even for the case of a large number of radial cracks $n = 40$, the absolute value of the relative error of the SIF predicted by G2CDD is lower than 4.2%, as compared to the relative errors of the other two methods that are greater or equal to 10%. From this analysis it

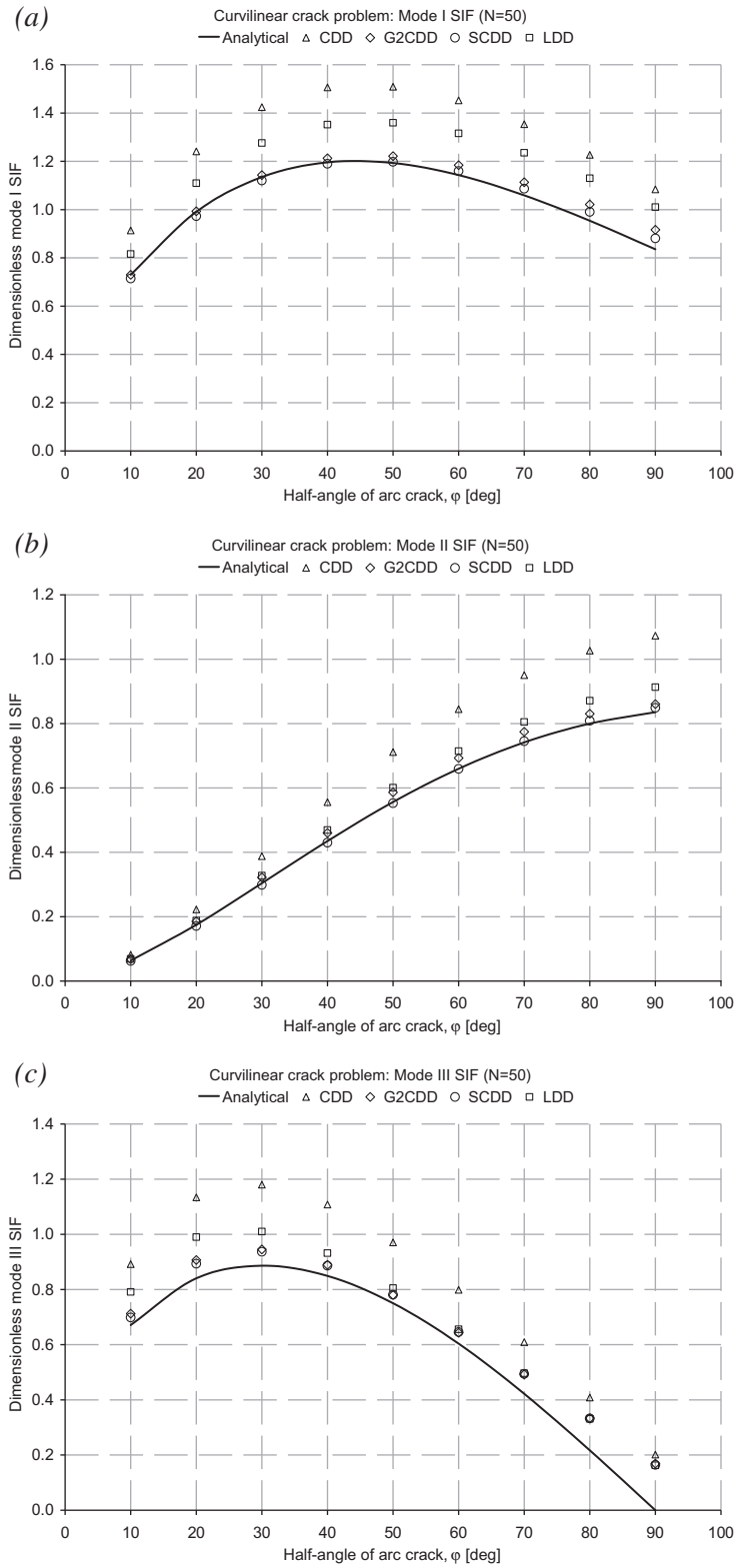

Fig. 9. Dependence of the SIFs (i.e. $K_i/(\sigma\sqrt{a})$, i = I, II, III) at the tip A of the arc crack on the half-arc angle φ for a fixed number of elements $N = 50$: (a) mode I, (b) mode II, and (c) mode III cases.

could be immediately observed: (a) the LDD method considerably reduces the error of the SIF compared to the CDD, and (b) the G2CDD method is always more accurate compared to LDD method and more efficient in terms of speed of calculations, since the linear displacement discontinuity pattern is represented by displacements at two element nodes whereas the G2 displacement discontinuity by only one node.

4.3. Case 3: The curvilinear crack problem

This case illustrated in Fig. 8 refers to the smooth arc crack, which is a part of a circle, in an isotropic infinite plane subjected to biaxial tension and anti-plane shear stress at infinity. The closed form expressions for the modes I, II and III SIFs at crack tip A are given as follows (Tada et al., 1973)

$$
\begin{aligned}
K_{I_A} &= \sigma\sqrt{\pi a \sin\varphi}\,\frac{\cos\frac{\varphi}{2}}{1+\sin^2\frac{\varphi}{2}},\\
K_{II_A} &= \sigma\sqrt{\pi a \sin\varphi}\,\frac{\sin\frac{\varphi}{2}}{1+\sin^2\frac{\varphi}{2}},\\
K_{III_A} &= \tau_l\sqrt{\pi a \sin\varphi}\left(\cos\frac{\varphi}{2}-\sin\frac{\varphi}{2}\right)\\
&= \sqrt{2}\tau_l\sqrt{\pi a \sin\varphi}\sin\left(\frac{\pi}{4}-\frac{\varphi}{2}\right).
\end{aligned}
\tag{19}
$$

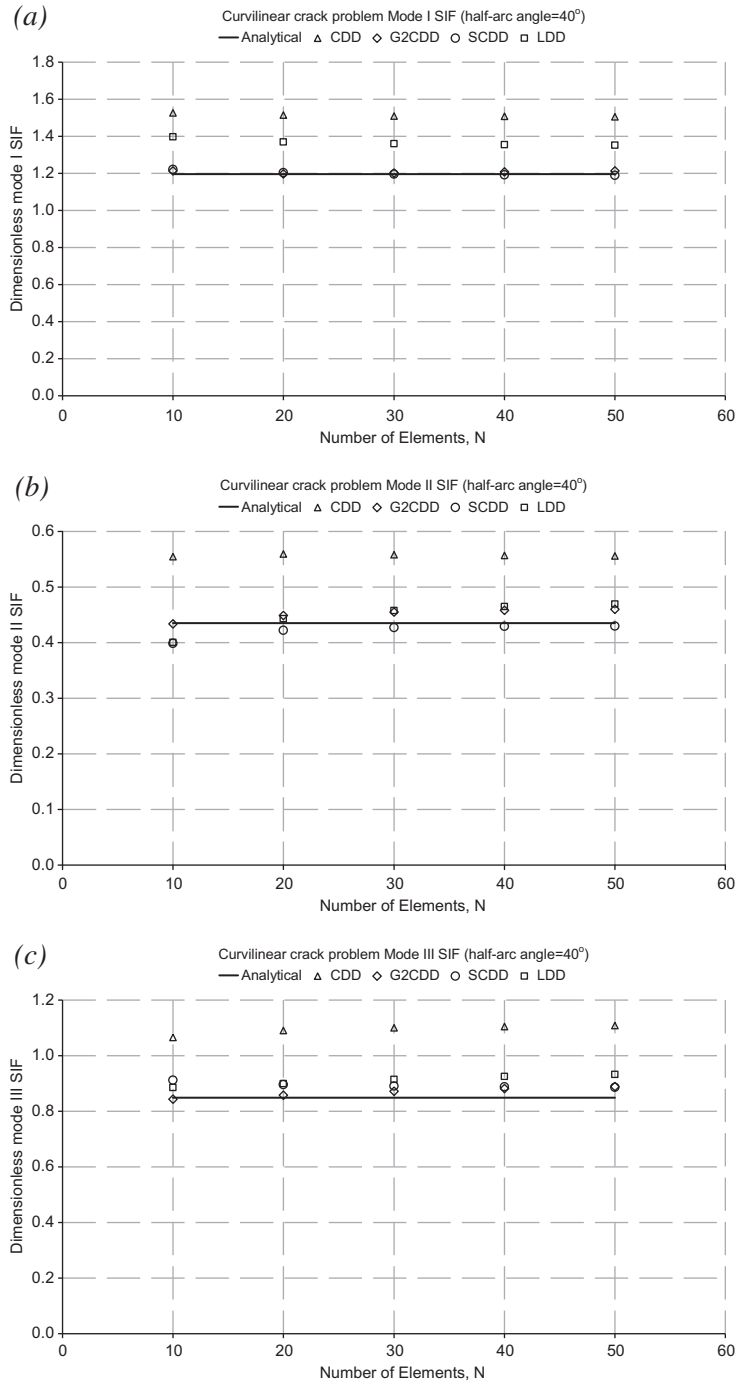

Fig. 10. Variation of the dimensionless SIFs (i.e. $K_i/(\sigma\sqrt{a})$, i = I, II, III) at the tip A of the arc crack with the number of elements for $\varphi = 40°$: (a) mode I, (b) mode II, and (c) mode III.

wherein φ stands for the half-angle of the sector prescribed by the crack, a is the radius of the circle, σdenotes the far-field biaxial tension, and $\tau_l$the far-field anti-plane shear stress.

In this particular problem, apart from the G2CDD, LDD and CDD methods, the special crack-tip displacement discontinuity (SCDD) element method (Shou and Crouch, 1995) was also implemented into G2TWODD code and applied for the numerical calculation of mode I, II and III SIFs. For the numerical implementation of the SCDD, the two special crack tip displacement discontinuity elements of each crack are placed locally at the corresponding left or right crack tips, while the rest of the elements that cover the crack apart from the tips are constant displacement discontinuity elements. It is worth noticing that the SCDD requires more computational effort than the G2CDD since in the former case the influence coefficients between the special crack tip elements and the CDD elements are given in integral form and should be calculated by virtue of Gauss quadrature (only in the case of straight cracks these integrals may be found analytically), while those of the latter are given in analytical form.

The graphical representations of the variation of modes I, II and III SIFs with the half-angle of the arc crack are also illustrated in Fig. 9a–c, respectively. From these figures it may be seen that the two methods, namely the G2CDD and SCDD, give always more closer results to the analytical solution than the other two numerical methods (i.e. CDD and LDD). It is also noted that for half-arc angles $\varphi \leqslant 30^\circ$, G2CDD gives the smaller relative error compared to all the other methods, whereas for higher values of the angle φ the SCDD gives slightly better predictions compared to G2CDD. It could be also remarked from this analysis that even for a small number of elements, i.e. $N = 10$ the G2CDD method is close to the analytical solution, while as the number of elements increases the numerical solution given by this method oscillates around the analytical one. Finally, Fig. 10a–c presents the variation of the normalized mode I SIF with the number of elements along the curvilinear crack for a constant half-arc angle equal to 40°.

5. Conclusions

In this work the G2CDD element was further elaborated for calculating the SIFs for general plane isotropic elasticity crack problems. A number of crack configurations were considered in order to compare the efficiency and accuracy of the G2, as well as of the constant, linear, and special crack tip DD elements. These examples show that the G2DD element is very efficient and more accurate for SIF calculations of complex plane cracks in infinite domains compared to the CDD and LDD elements. Also, the proposed element has comparable accuracy with the SCDD element, but it is more efficient since it avoids extra numerical integrations for the calculation of the influence coefficients. Hence, the use of this element allows accurate analysis of a crack tip without recourse to a special crack tip element or elements with more than one collocation points (e.g. linear), and makes the DD method suitable for the solution of crack problems. The method can be extended to cope with the interaction of cracks of arbitrary shape with a free surface (i.e. the half-plane problem). This extension of the method is presented in Part II (Exadaktylos and Xiroudakis, submitted for publication).

References

Chen, J.T., Hong, H.-K., 1999. Review of dual boundary element methods with emphasis on hypersingular integrals and divergent series. Appl. Mech. Rev. 52 (1), 17–33.

Crawford, A.M., Curran, J.H., 1982. Higher-order functional variation displacement discontinuity elements. Int. J. Rock Mech. Min. Sci. Geomech. Abstr. 19, 143–148.

Crouch, S.L., 1976a. Analysis of stresses and displacements around underground excavations: an application of the Displacement Discontinuity Method. University of Minnesota Geomechanics Report, Minneapolis, Minnesota, November, 1976.

Crouch, S.L., 1976b. Solution of plane elasticity problems by the displacement discontinuity method. Int. J. Numer. Methods Eng. 10, 301–343.

Crouch, S.L., Starfield, A.M., 1990. Boundary Element Methods in Solid Mechanics. Unwin Hyman, Boston.

Exadaktylos, G., 1998. Gradient elasticity with surface energy: Mode-I crack problem. Int. J. Solids Struct. 35 (5–6), 421–456.

Exadaktylos, G., 1999. Some basic half-plane problems of the cohesive elasticity theory with surface energy. Acta Mech. 133 (1–4), 175–198.

Exadaktylos, G., Aifantis, E., 1996. Two and three dimensional crack problems in gradient elasticity. J. Mech. Beh. Mtls. 7 (2), 93–117.

Exadaktylos, G., Vardoulakis, I., 2001. Microstructure in linear elasticity and scale effects: a reconsideration of basic rock mechanics and rock fracture mechanics. Tectonophysics 335 (1–2), 81–110.

Exadaktylos, G., Xiroudakis, G., 2010a. A G2 constant displacement discontinuity element for analysis of crack problems. Comput. Mech. 45, 245–261.

Exadaktylos, G., Xiroudakis, G., submitted for publication. The G2 constant displacement discontinuity method – Part II: Solution of half-plane crack problems. Int. J. Solids Struct.

Exadaktylos, G., Vardoulakis, I., Aifantis, E., 1996. Cracks in gradient elastic bodies with surface energy. Int. J. Fract. 79, 107–119.

Gradshteyn, I.S., Ryzhik, I.M., 1980. In: Jeffrey, Allan (Ed.), Tables of Integrals, Series, and Products, corrected and enlarged edition. Academic Press.

Hong, H.-K., Chen, J.T., 1988a. Derivations of integral equations of elasticity. J. Eng. Mech. 114 (6), 1028–1044.

Hong, H.-K., Chen, J.T., 1988b. Generality and special cases of dual integral equations of elasticity. J. Chinese Soc. Mech. Eng. 9 (1), 1–9.

Shou, K.J., Crouch, S.L., 1995. A higher order displacement discontinuity method for analysis of crack problems. Int. J. Rock Mech. Min. Sci. Geomech. Abstr. 32/1, 49–55.

Sneddon, I.N., Lowengrub, M., 1969. Crack Problems in the Classical Theory of Elasticity. John Wiley & Sons, Inc., New York.

Tada, H., Paris, P., Irwin, G., 1973. The Stress Analysis of Cracks Handbook. Del Research Corporation, Hellertown, Pennsylvania. pp. 2.1–2.5.

Vardoulakis, I., Exadaktylos, G., Aifantis, E., 1996. Gradient elasticity with surface energy: Mode III crack problem. Int. J. Solids Struct. 33 (30), 4531–4559.